Title

Interplay between Disulfide Bonding and N-Glycosylation Defines SLC4 Na+-coupled Transporter Extracellular Topography*

Journal

Journal of Biological Chemistry, 290(9)

ISSN

0021-9258

Authors

Zhu, Quansheng
Kao, Liyo
Azimov, Rustam
et al.

Publication Date

2015-02-01

DOI

10.1074/jbc.m114.619320

Peer reviewed

THE JOURNAL OF BIOLOGICAL CHEMISTRY VOL. 290, NO. 9, pp. 5391–5404, February 27, 2015

Interplay between Disulfide Bonding and *N*-Glycosylation Defines SLC4 Na^+-coupled Transporter Extracellular Topography*

Received for publication, October 15, 2014, and in revised form, November 25, 2014 Published, JBC Papers in Press, January 8, 2015, DOI 10.1074/jbc.M114.619320

Quansheng Zhu[‡1], **Liyo Kao**[‡], **Rustam Azimov**[‡], **Natalia Abuladze**[‡], **Debra Newman**[‡], **and Ira Kurtz**[‡§]

From the [‡]*Department of Medicine and* [§]*Brain Research Institute, David Geffen School of Medicine, UCLA, Los Angeles, California 90095-1689*

Background: Cysteines in extracellular loop 3 (EL-3) are highly conserved in SLC4 Na^+-coupled transporters.
Results: Disulfide bonding and *N*-glycosylation uniquely determine the topography of NBCe1-A EL-3.
Conclusion: A domain-like structure formed by EL-3 is present at the NBCe1-A dimeric interface.
Significance: The interplay between disulfide bonding and *N*-glycosylation may play an important role in transmembrane protein maturation.

The extracellular loop 3 (EL-3) of SLC4 Na^+-coupled transporters contains 4 highly conserved cysteines and multiple *N*-glycosylation consensus sites. In the electrogenic Na^+-HCO_3^- cotransporter NBCe1-A, EL-3 is the largest extracellular loop and is predicted to consist of 82 amino acids. To determine the structural-functional importance of the conserved cysteines and the *N*-glycosylation sites in NBCe1-A EL-3, we analyzed the potential interplay between EL-3 disulfide bonding and *N*-glycosylation and their roles in EL-3 topological folding. Our results demonstrate that the 4 highly conserved cysteines form two intramolecular disulfide bonds, Cys^{583}-Cys^{585} and Cys^{617}-Cys^{642}, respectively, that constrain EL-3 in a folded conformation. The formation of the second disulfide bond is spontaneous and unaffected by the *N*-glycosylation state of EL-3 or the first disulfide bond, whereas formation of the first disulfide bond relies on the presence of the second disulfide bond and is affected by *N*-glycosylation. Importantly, EL-3 from each monomer is adjacently located at the NBCe1-A dimeric interface. When the two disulfide bonds are missing, EL-3 adopts an extended conformation highly accessible to protease digestion. This unique adjacent parallel location of two symmetrically folded EL-3 loops from each monomer resembles a domain-like structure that is potentially important for NBCe1-A function *in vivo*. Moreover, the formation of this unique structure is critically dependent on the finely tuned interplay between disulfide bonding and *N*-glycosylation in the membrane processed NBCe1-A dimer.

SLC4 transporters represent a family of membrane proteins that transport HCO_3^- in various cell types (1–3). These transporters are widely expressed in the brain, heart, kidney, pancreas, intestine, muscle, teeth, and eye where they play critical roles in intracellular pH regulation, transepithelial transport, and systemic acid-base balance. SLC4 transporters have high amino acid sequence homology but vary in their Na^+ and Cl^- dependence, stoichiometry (electroneutral/electrogenic), and mechanisms of ion transport (exchanger/cotransporter) (1–3).

Of all the SLC4 Na^+-coupled transporters, the electrogenic Na^+-base cotransporter NBCe1 has been studied extensively because of its essential role in mediating HCO_3^- transport in multiple organs including kidney, brain, eye, and tooth ameloblasts (1–3). Eight missense mutations in NBCe1 have thus far been reported to cause a severe form of human proximal renal tubular acidosis with extrarenal manifestations (1, 4). These mutations affect NBCe1 structure-function properties and membrane expression (1, 4, 5). A naturally occurring missense mutation, T485S, was recently shown to affect the electrogenicity of NBCe1, switching the mode of transport from Na^+-CO_3^{2-} to Na^+-HCO_3^- cotransport (6).

The human *SLC4A4* gene encodes three NBCe1 protein variants (-A, -B, and -C), and additional transcripts (-D and -E) have been reported in mouse (7–9). These variants differ in their N- and C-terminal regions but have the identical transmembrane region (8). NBCe1-A exists as a homodimer in the plasma membrane with each monomer functioning independently (10). Each monomer consists of an N-terminal cytoplasmic region, a C-terminal transmembrane region, and a short C-terminal cytoplasmic tail. The N-terminal cytoplasmic region is in a folded conformation and interacts tightly with the transmembrane region (11, 12), and the C-terminal cytoplasmic tail contains motifs that are critical for NBCe1-A membrane trafficking (13–15). Interestingly, the C-terminal tails from each monomer are closely associated in the cytosol, suggesting that they may have additional roles for NBCe1-A function (16). The transmembrane region of NBCe1-A contains 14 transmembrane segments (TMs)[2] with TM1, -3, and -8 involved in forming the

* This work was supported, in whole or in part, by National Institutes of Health Grant DK077162 (to I. K.). This work was also supported by a Norman S. Coplon Grant from Satellite Healthcare (to Q. Z.) and by the Factor Family Foundation, the Allan Smidt Charitable Fund, and the Arvey Foundation (to I. K.).
[1] To whom correspondence should be addressed: Dept. of Medicine, UCLA, 7-155 Factor Bldg., 10833 Le Conte Ave., Los Angeles, CA 90095-1689. Tel.: 310-206-6741; Fax: 310-825-6309; E-mail: quzhu@mednet.ucla.edu.

[2] The abbreviations used are: TM, transmembrane segment; BM, biotin maleimide, 3-(*N*-maleimidylpropionyl)biocytin; BCECF-AM, 2′,7′-bis(2-carboxyethyl)-5(6)-carboxyfluorescein tetrakis(acetoxymethyl) ester; DIDS, 4,4′-diisothiocyanato-2,2′-stilbenedisulfonic acid; EL-3, extracellular loop 3; Endo, endoglycosidase; NHS, *N*-hydroxysuccinimide; β-ME, β-mercaptoethanol; $5C^-$, NBCe1-A-$5C^-$; $9C^-$, NBCe1-A-$9C^-$; C1035, NBCe1-A-C1035; C642, NBCe1-A-C642; $2N^-$-$5C^-$, NBCe1-A-$5C^-$-N597Q/N617Q; Ab, antibody.

ion permeation pathway (6, 17, 18) and TM10–14 forming a scaffold structure to accommodate the ion interaction site (12) (see Fig. 1*A*).

Sequence alignment analysis reveals that a common structural feature exists among all SLC4 Na^+-coupled transporters: a large extracellular loop 3 (EL-3) with multiple *N*-glycosylation consensus sites and 4 highly conserved cysteines (see Fig. 1*B*). In NBCe1-A, this loop is predicted to contain 82 amino acids (5) with three *N*-glycosylation consensus sites (Asn^{592}, Asn^{597}, and Asn^{617}) of which only two (Asn^{597} and Asn^{617}) are glycosylated (19). The *N*-glycosylation of EL-3 is predicted to be important for NBCe1-A plasma membrane trafficking, whereas the role of the 4 highly conserved cysteines in EL-3 has remained unclear. In the human organic cation transporter 2, cysteines in the extracellular loops play a crucial role in protein plasma membrane trafficking and are involved in transporter oligomerization (20). Moreover, in Cys-loop ligand-gated ion channel receptors, the disulfide bonds in a large extracellular loop are involved in forming the substrate interaction site (21). The TM prior to NBCe1-A EL-3 (TM5) contains a charged peptide motif ^{558}KKMIK^{562} that forms one of the DIDS (an NBCe1-A functional inhibitor) binding sites (22). A single amino acid substitution, D555E in TM5, was shown to convert NBCe1-A from a cotransporter to an anion channel (23). Taken together, EL-3 may have an important structure-function role in NBCe1-A ion transport.

In the present study, we determined that the 4 cysteines in NBCe1-A EL-3 form two intramolecular disulfide bonds that constrain EL-3 in a folded conformation. Our results also demonstrated that EL-3 from each monomer resides closely at the NBCe1-A dimeric interface, forming a unique topological structure. Moreover, our data have shown for the first time that in a transmembrane protein, a unique interplay exists between disulfide bonding and *N*-glycosylation that governs the topological folding of a large extracellular loop.

EXPERIMENTAL PROCEDURES

Materials—Site-directed mutagenesis kits were from Stratagene. Biotin maleimide, BCECF-AM, DIDS, DMEM, and all cell culture reagents were from Invitrogen. Protein A-Sepharose, streptavidin-biotinylated horseradish peroxidase (HRP) complex and goat anti-rabbit IgG-conjugated horseradish peroxidase were from GE Healthcare. Endo-F (peptide-*N*-glycosidase F) and Endo-H were from New England Biolabs. NHS-SS-biotin and streptavidin-agarose beads were from Thermo Scientific. Igepal, polylysine, chymotrypsin, cycloheximide, and nigericin were from Sigma. PVDF membrane was from Millipore.

Site-directed Mutagenesis—A wild-type human NBCe1-A cDNA was used as the template for site-directed mutagenesis. Mutagenesis was performed using the Stratagene site-directed mutagenesis kit following the manufacturer's protocol. The complete cDNA sequence of each construct was verified by DNA sequencing.

Protein Expression—Mutant NBCe1-A proteins were transiently expressed in human embryonic kidney 293 (HEK 293) cells by using Lipofectamine 2000 transfection following the manufacturer's protocol. Cells were grown at 37 °C in a 5% CO_2 atmosphere and harvested 24–48 h post-transfection.

Immunocytochemistry—24 h post-transfection, cells were rinsed with PBS (140 mM NaCl, 3 mM KCl, 6.5 mM Na_2HPO_4, 1.5 mM KH_2PO_4, pH 7.4) and incubated with a rabbit anti-human NBCe1-A antibody (Ab-162; 1:100 dilutions in PBS). After a 15-min incubation at room temperature, the cells were rinsed with PBS and further incubated with goat anti-rabbit IgG conjugated with Cy3 (Jackson ImmunoResearch Laboratories; 1:500 dilution in PBS) for 30 min. The cells were then rinsed three times with PBS and mounted in Crystal/Mount (Biomeda, Foster City, CA). In some experiments, transfected cells were permeabilized with 1 ml of ice-cold methanol for 2 min prior to the immunostaining or were treated with 0.01 mg/ml chymotrypsin in digestion buffer (140 mM NaCl, 10 mM $CaCl_2$, 20 mM HEPES, pH 7.8) for 5 min at 37 °C prior to Ab-162 staining. Fluorescence images were acquired by a PXL charge-coupled device camera (model CH1, Photometrics) coupled to a Nikon Microphot-FXA epifluorescence microscope. All constructs used in the study were analyzed by Ab-162 immunostaining and were shown to be expressed on the plasma membrane.

Functional Transport Assay of NBCe1-A—HEK 293 cells grown on coated coverslips were transfected with NBCe1-A mutant cDNAs using Lipofectamine 2000. 24 h post-transfection, cells were loaded with fluorescent pH probe BCECF-AM and assayed using a microfluorometer as described previously (17).

Biotin Maleimide Labeling and Immunoprecipitation—Whole cell labeling with biotin maleimide was performed as described previously (17). Briefly, transfected HEK 293 cells were collected in PBSCM (PBS containing 0.1 mM $CaCl_2$, 1 mM $MgCl_2$, pH 7.0) and labeled with 0.2 mM biotin maleimide for 10 min at room temperature. The cells were then lysed in 500 μl of immunoprecipitation buffer (5 mM EDTA, 150 mM NaCl, 1% (v/v) Igepal, 0.5% (w/v) sodium deoxycholate, 10 mM Tris-HCl, pH 7.5) containing 0.2% (w/v) bovine serum albumin and protease inhibitors (Roche Applied Science), and NBCe1-A protein was immunoprecipitated using a rabbit anti-human NBCe1-A N terminus polyclonal antibody (24) and protein A beads.

SDS-PAGE and Immunoblotting—Protein samples were eluted in 2× SDS sample buffer containing 2% β-ME, resolved on 7.5% polyacrylamide gels, and transferred to PVDF membranes. Biotinylated proteins were detected by incubation of blots with 1:10,000 diluted streptavidin-biotinylated horseradish peroxidase (GE Healthcare) in TBSTB buffer (TBST buffer (0.1% (v/v) Tween 20, 137 mM NaCl, 20 mM Tris, pH 7.5) containing 0.5% (w/v) bovine serum albumin). The protein expression level was determined by probing the stripped blots with an anti-NBCe1 C terminus polyclonal antibody (12) at 1:3000 dilutions in TBSTM buffer (TBST buffer containing 5% (w/v) nonfat milk).

Plasma Membrane Stripping—Cell membranes were isolated in hypotonic solution (10 mM Tris, 2 mM EDTA, pH 7.5). Membrane treatment with Na_2CO_3 was performed as described previously (5, 12). Briefly, isolated cell membranes were resuspended in 100 μl of 1% sucrose solution and incubated with 2

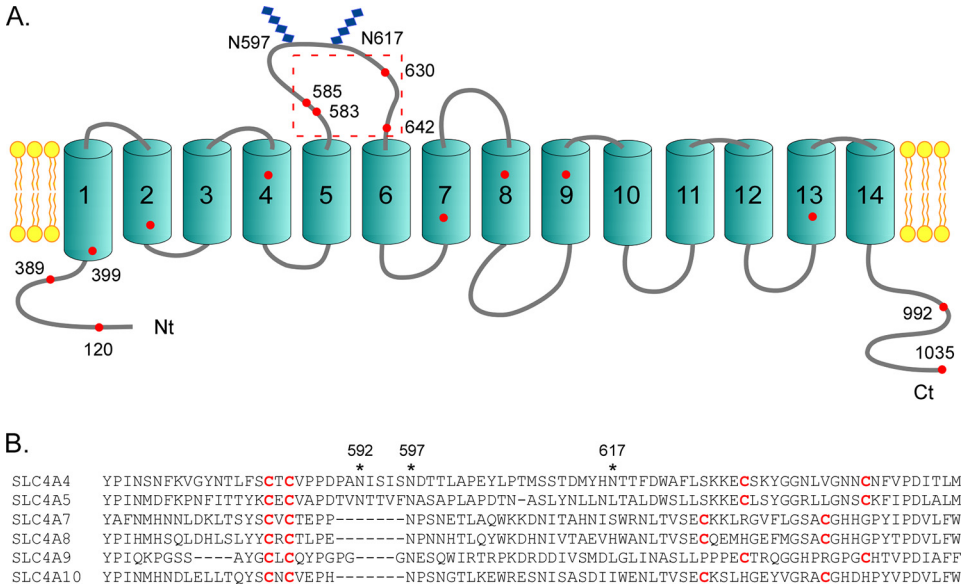

FIGURE 1. **Topology of NBCe1-A and sequence alignment of the predicted EL-3 among SLC4 Na^+-HCO_3^- cotransporters.** *A*, the NBCe1-A topology was proposed based on our recent and previous reports (5, 11, 12). The branched structures at Asn^{597} and Asn^{617} represent *N*-linked glycosylation. Locations of the 15 endogenous cysteines are indicated as *filled red circles*. *Square* marks the 4 highly conserved cysteines in EL-3. The N (*Nt*) and C (*Ct*) termini are marked. TMs are numbered *1–14*. *B*, amino acid sequences of NBCe1-A and SLC4 Na^+-HCO_3^- transporters were aligned using the ClustalW program. The 4 highly conserved cysteines are colored in *red*. *Asterisks* indicate the potential *N*-glycosylation sites in NBCe1-A EL-3.

ml of 0.1 or 1 M of Na_2CO_3 at 4 °C on a rotating shaker for 30 min. Membranes were then pelleted, washed three times with PBS, pH 7.0 and equilibrated in PBSCM, pH 7.0 prior to biotin maleimide (BM) labeling.

NBCe1-A Membrane Stability Assay—24 h post-transfection, cells expressing WT-NBCe1-A or NBCe1-A lacking the 4 cysteines in EL-3 were exposed to cycloheximide (10 μM) (to suppress protein synthesis) (25) in fresh cell culture medium. At 0, 24, 48, 72, and 96 h post-cycloheximide treatment, the cells were rinsed with PBS and incubated with sulfo-NHS-SS-biotin for 30 min at 4 °C following the manufacturer's protocol. The cells were then collected, lysed, and immunoprecipitated with streptavidin-agarose beads. Protein samples were eluted with SDS sample buffer containing 2% β-ME, resolved by SDS-PAGE, and detected with a rabbit anti-human NBCe1-A antibody.

NBCe1-A Deglycosylation Analysis—48 h post-transfection, cells expressing various NBCe1-A constructs were collected, and cell membranes were isolated as described above. The isolated cell membranes were then resuspended in Endo-F or Endo-H digestion buffer and processed following the manufacturer's protocol. Protein samples were resolved by SDS-PAGE and detected with a rabbit anti-human NBCe1-A antibody.

Image and Data Analysis—Films from immunoblots and biotinylation blots were scanned with a Hewlett-Packard Scanjet 5590. Scanned images were quantified with UN-SCAN-IT gel™ Version 6.1 software. Biotinylation levels were calculated according to Ref. 26.

Statistical Analysis—Means ± S.E. were calculated with SigmaPlot 10 software. Statistical analysis was performed using SigmaPlot 10 software. Dunnett's *t* test was used to assess statistical significance with $p < 0.05$ considered significant.

RESULTS

The Cysteines in NBCe1-A EL-3 Form Intramolecular Disulfide Bonds

Identification of Aqueous Accessible Cysteines in NBCe1-A—Wild-type NBCe1-A (WT-NBCe1-A) contains 15 endogenous cysteines of which 5 are located in the cytoplasmic regions and 4 are located in EL-3 that are potentially exposed to the aqueous environment (Fig. 1*A*). To determine whether one or more of these cysteines are accessible to the intra- or extracellular medium, we engineered a construct with the 5 cytoplasmic cysteines substituted with serines (NBCe1-A-5C$^-$). By using this construct as a template, we individually reintroduced each of the 5 substituted cysteines. Aqueous accessibility of the reintroduced cysteines was assessed by BM labeling; BM is a reagent that only reacts with aqueous exposed sulfhydryl groups on the surface of a protein (27). Fig. 2*A* shows that WT-NBCe1-A was strongly labeled, whereas NBCe1-A-5C$^-$ had no labeling. Cys^{389}, Cys^{992}, and Cys^{1035} were labeled, whereas Cys^{120} and Cys^{399} were not labeled, indicating that the latter two are buried in the N-terminal cytoplasmic region of NBCe1-A. The lack of BM labeling of NBCe1-A-5C$^-$ suggests that the 4 cysteines in EL-3 (Cys^{583}, Cys^{585}, Cys^{630}, and Cys^{642}) either form intra- or intermolecular disulfide bonds or are tightly folded in NBCe1-A EL-3.

Cysteines in EL-3 Form Intramolecular Disulfide Bonds—To determine this, we expressed NBCe1-A-5C$^-$ in HEK 293 cells and compared protein migration on SDS-PAGE under nonreducing and reducing conditions. Fig. 2*B* shows that the nonreduced NBCe1-A-5C$^-$ protein migrated as a protein band around 140 kDa on SDS-PAGE, ruling out that the 4 cysteines in EL-3 form intermolecular disulfide bonds in the NBCe1-A dimer. When NBCe1-A-5C$^-$ was reduced, the protein migrated as a lower molecular weight band, indicating that a

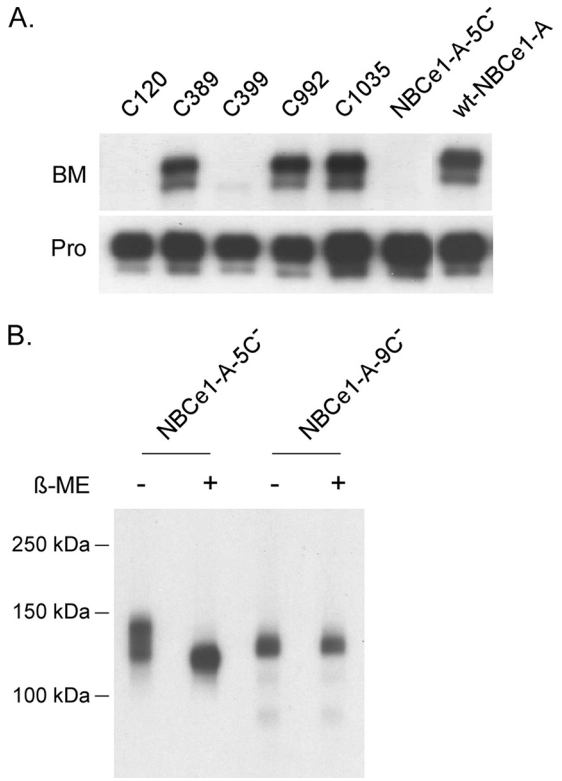

FIGURE 2. **BM labeling of NBCe1-A cysteine-reintroduced constructs and detection of intramolecular disulfide bonds in NBCe1-A.** *A*, representative data of BM labeling. HEK 293 cells expressing individual cysteine-reintroduced constructs were labeled with BM at room temperature. Cells were lysed, and NBCe1-A protein was immunoprecipitated, resolved by 7.5% SDS-PAGE, and transferred to a PVDF membrane. Incorporated biotin was detected by HRP-streptavidin and ECL. Blots were stripped and probed with an anti-NBCe1 antibody to detect the amount of NBCe1-A protein in each sample. *Pro*, protein. *B*, the β-ME-treated and untreated NBCe1-A-5C$^-$ and NBCe1-A-9C$^-$ protein samples were resolved by 7.5% SDS-PAGE, transferred to a PVDF membrane, and probed with an anti-NBCe1-A antibody. −, without β-ME; +, with β-ME.

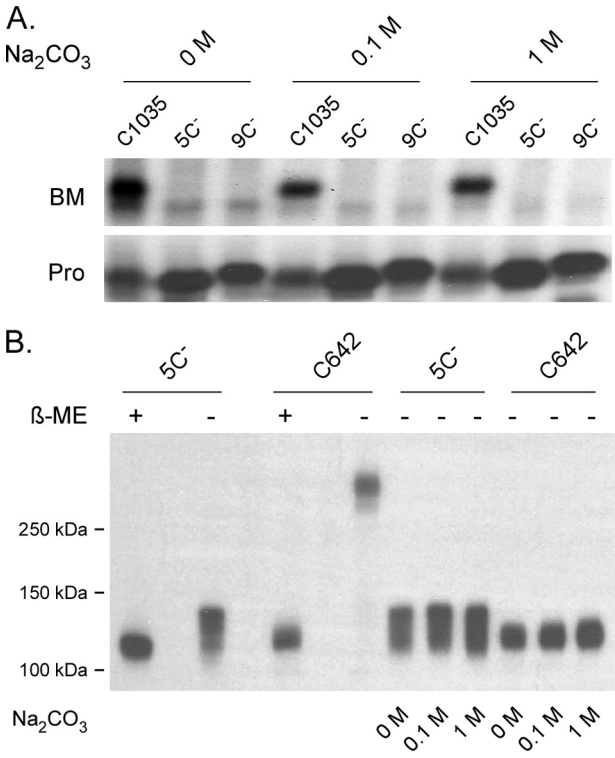

FIGURE 3. **Effect of Na_2CO_3 treatment on surface exposure of the intramolecular disulfide bonds in EL-3.** *A*, plasma membranes isolated from HEK 293 cells expressing C1035, 5C$^-$, or 9C$^-$ were stripped with 0, 0.1, or 1 M Na_2CO_3 at 4 °C for 30 min followed with 50 mM DTT treatment at 37 °C prior to BM labeling. *Pro*, protein. *B*, Na_2CO_3- and DTT-treated 5C$^-$ and C642 were resolved by 7.5% SDS-PAGE without β-ME treatment. C642 contains only one cysteine (Cys^{642}) in EL-3 that forms an intermolecular disulfide bond with itself on the opposite monomer to form a dimer.

structural constraint in NBC1-A-5C$^-$ mediated by intramolecular disulfide bond(s) was removed. To determine whether the 4 cysteines in EL-3 are responsible for the increased migration of reduced NBCe1-A, we substituted all 4 cysteines with serines (NBCe1-A-9C$^-$) and resolved the protein by SDS-PAGE. Fig. 2*B* shows that β-ME treatment had no effect on NBCe1-A-9C$^-$ migration in contrast to NBCe1-A-5C$^-$, indicating that the 4 cysteines in EL-3 form intramolecular disulfide bonds. Interestingly, NBCe1-A-9C$^-$ migrated as a high molecular weight band compared with NBCe1-A-5C$^-$, suggesting that the normally unglycosylated site in EL-3 (Asn^{592}) became glycosylated when disulfide bonds were absent.

The Disulfide Bonds in EL-3 Are Buried in the NBCe1-A Protein Complex, Constraining EL-3 in a Folded Conformation

We next tested whether the disulfide bonds in EL-3 could be freed by DTT treatment. Plasma membranes from HEK 293 cells expressing NBCe1-A-5C$^-$ (5C$^-$), NBCe1-A-9C$^-$ (9C$^-$), or NBCe1-A-C1035 (C1035) were isolated and treated with 50 mM DTT prior to BM labeling. Fig. 3*A* shows the positive control C1035 strongly labeled; the negative control 9C$^-$ had no labeling. Surprisingly, 5C$^-$ also was unlabeled after the treatment, indicating that the reducing reagents failed to free the cysteines in EL-3. We then attempted to expose the disulfide bonds in EL-3 by stripping the isolated membranes with 0.1 M or 1 M Na_2CO_3, pH 12 followed with 50 mM DTT treatment and BM labeling. Again, the result showed that none of the 4 cysteines in EL-3 were freed (Fig. 3*A*). To further confirm that the disulfide bonds in EL-3 remained intact after these treatments, we resolved the proteins by SDS-PAGE under nonreducing conditions. Fig. 3*B* shows that the disulfide bonds in 5C$^-$ were not reduced even after 1 M Na_2CO_3 treatment in contrast to the positive control (Cys^{642}) whose intermolecular disulfide bond was completely reduced. Taken together, our data indicate that the disulfide bonds in EL-3 are not exposed on the extracellular surface of NBCe1-A.

To determine how the disulfide bonds shape the EL-3 conformation, we tested the accessibility of EL-3 to chymotrypsin digestion in the presence or absence of the 4 cysteines. Transfected HEK 293 cells were incubated briefly with chymotrypsin (5 min) and subsequently stained with an antibody (Ab-162) that specifically recognizes the peptide between the two *N*-glycosylated sites, Asn^{597} and Asn^{617}, in EL-3. Fig. 4*A* shows that chymotrypsin treatment completely eliminated the epitope for Ab-162 staining in 9C$^-$ but had no effect on Ab-162 staining of 5C$^-$, indicating that in the absence of the disulfide bonds, EL-3 adopts an extended conformation highly accessible to protease digestion. Chymotryptic digestion was then verified by immunoblotting (Fig. 4*B*), which showed that a distinct N-terminal peptide and a C-terminal peptide were released from 9C$^-$ but

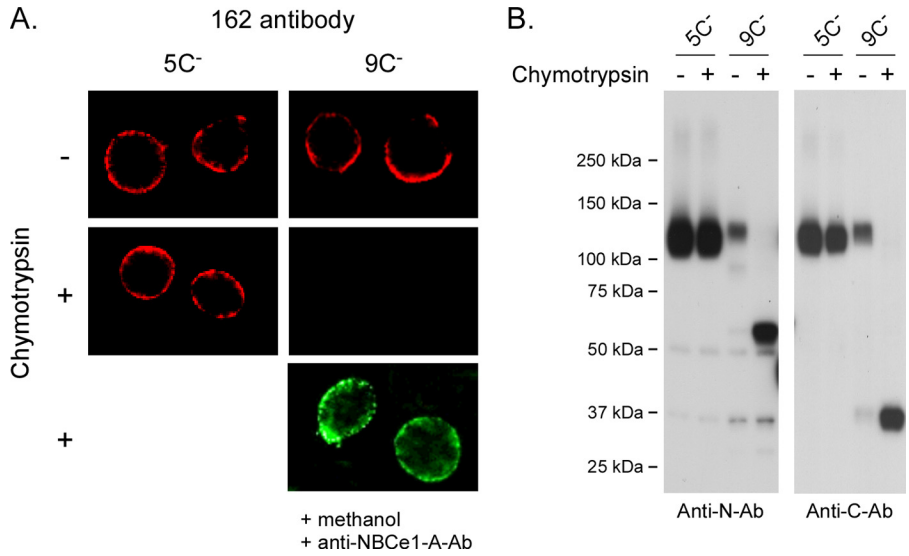

FIGURE 4. **Chymotrypsin treatment of 5C$^-$ and 9C$^-$.** *A*, HEK 293 cells expressing 5C$^-$ and 9C$^-$ were briefly incubated with chymotrypsin (5 min) at 37 °C. Cells were subsequently washed with PBS and incubated with Ab-162 that specifically recognizes the peptide between Asn^{597} and Asn^{617} for 15 min at room temperature. The fluorescence images were acquired by a PXL charge-coupled device camera coupled to a Nikon Microphot-FXA epifluorescence microscope. The Ab-162-negative stained cells were then permeabilized with methanol and incubated with a rabbit anti-human NBCe1-A N terminus polyclonal antibody. *B*, cell membranes from chymotrypsin-treated HEK 293 cells were isolated and lysed in immunoprecipitation buffer. Insoluble materials were removed by centrifugation at full speed for 30 min. Protein samples were then resolved by 7.5% SDS-PAGE, blotted to a PVDF membrane, and probed by an anti-NBCe1-A N or C terminus antibody, respectively. −, without chymotrypsin; +, with chymotrypsin.

TABLE 1
Cysteine combinations constructed in NBCe1-A EL-3
All the combinations were constructed using NBCe1-A-5C$^-$ as the template.

Number	Cysteine substitutions	Remaining cysteine combinations
1	C583S	Cys^{585}/Cys^{630}/Cys^{642}
2	C585S	Cys^{583}/Cys^{630}/Cys^{642}
3	C630S	Cys^{583}/Cys^{585}/Cys^{642}
4	C642S	Cys^{583}/Cys^{585}/Cys^{630}
5	C583S/C585S	Cys^{630}/Cys^{642}
6	C630S/C642S	Cys^{583}/Cys^{585}
7	C583S/C642S	Cys^{585}/Cys^{630}
8	C585S/C642S	Cys^{583}/Cys^{630}
9	C585S/C630S/C642S	Cys^{583}
10	C583S/C630S/C642S	Cys^{585}
11	C583S/C585S/C642S	Cys^{630}
12	C583S/C585S/C630S	Cys^{642}

not from 5C$^-$, indicating that cleavage only occurred in EL-3 when the cysteines were absent. These results demonstrate clearly that the disulfide bonds in EL-3 constrain the loop in a folded conformation on the NBCe1-A extracellular surface.

The Pattern of Disulfide Bonding among the 4 Cysteines in NBCe1-A EL-3

To determine how the disulfide bonds are formed among the 4 cysteines in EL-3, we engineered 12 constructs with different cysteine combinations in EL-3 using 5C$^-$ as the template (Table 1). We predicted that if one or more of the cysteines in EL-3 are substituted with serines, then the unpaired cysteines would be freely available for BM labeling. Surprisingly, after a 10-min incubation with BM, only two of the cysteine substituted combinations were moderately labeled (Fig. 5*A*). We reasoned that the negative data may have resulted from intermolecular cross-linking of the unpaired cysteines on each of the NBCe1-A monomers and therefore treated the transfected HEK 293 with 5 mM DTT followed with BM labeling. Indeed, Fig. 5*B* shows that DTT treatment freed the cross-linked cysteines, resulting in their subsequent labeling by BM.

To further determine whether intermolecular cross-linking occurred between the unpaired EL-3 cysteines in the NBCe1-A dimer, we resolved each of the cysteine substituted combinations by SDS-PAGE under both nonreducing and reducing conditions. Fig. 5*C* shows that all the cysteine combinations formed β-ME-sensitive dimers on SDS-PAGE except the Cys$^{630/642}$ combination, indicating that the unpaired cysteines are intermolecularly cross-linked and that the Cys$^{630/642}$ pair normally forms a native disulfide bond. Fig. 5*D* summarizes the results of BM labeling of all the cysteine combinations without or with DTT pretreatment and the efficiency of cross-linking. The native disulfide bonding between Cys^{630} and Cys^{642} indicates that Cys^{583} and Cys^{585} form a disulfide bond in wild-type NBCe1-A. Noticeably, when Cys$^{583/642}$ or Cys$^{585/642}$ were present, the cysteines were moderately labeled by BM, and fewer dimers were formed, further supporting that Cys^{630} and Cys^{642} and that Cys^{583} and Cys^{585} form disulfide bonds, respectively.

Interestingly, we observed that NBCe1-A lacking Cys^{583} and Cys^{585} migrated significantly more slowly compared with 5C$^-$ on SDS-PAGE under the reducing condition (Fig. 5*B*). To further confirm this, we resolved the NBCe1-A constructs with either single or double cysteines in EL-3 by 7.5% SDS-PAGE for an extended period of time. Fig. 5*E* shows that when Cys^{583}, Cys^{585}, or both were present NBCe1-A migrated at the same molecular weight position as 5C$^-$; however, when Cys^{583} and Cys^{585} were both absent, NBCe1-A migrated at the same molecular weight position as 9C$^-$. This result suggests that simultaneous removal of Cys^{583} and Cys^{585} induced glycosylation at Asn^{592}.

Effect of N-Glycosylation on Disulfide Bonding in NBCe1-A EL-3

NBCe1-A EL-3 contains three *N*-glycosylation consensus sites, but only two were reported to be glycosylated in *Xenopus* oocytes, and removal of all the three consensus sites had no

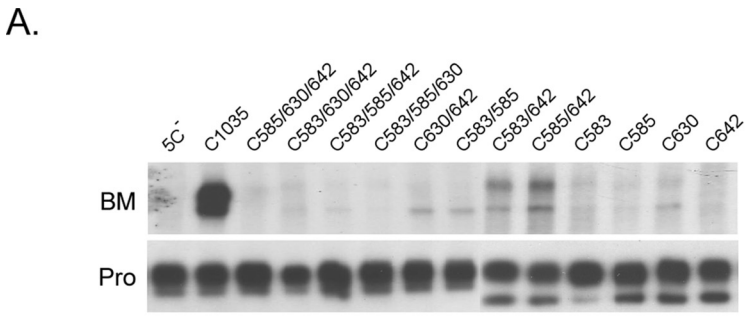

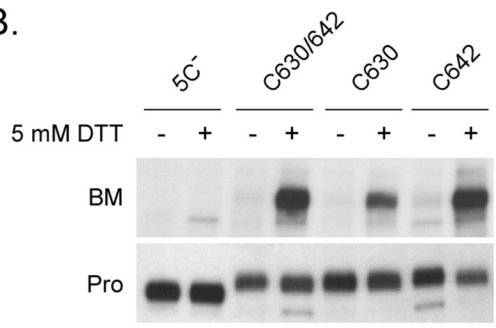

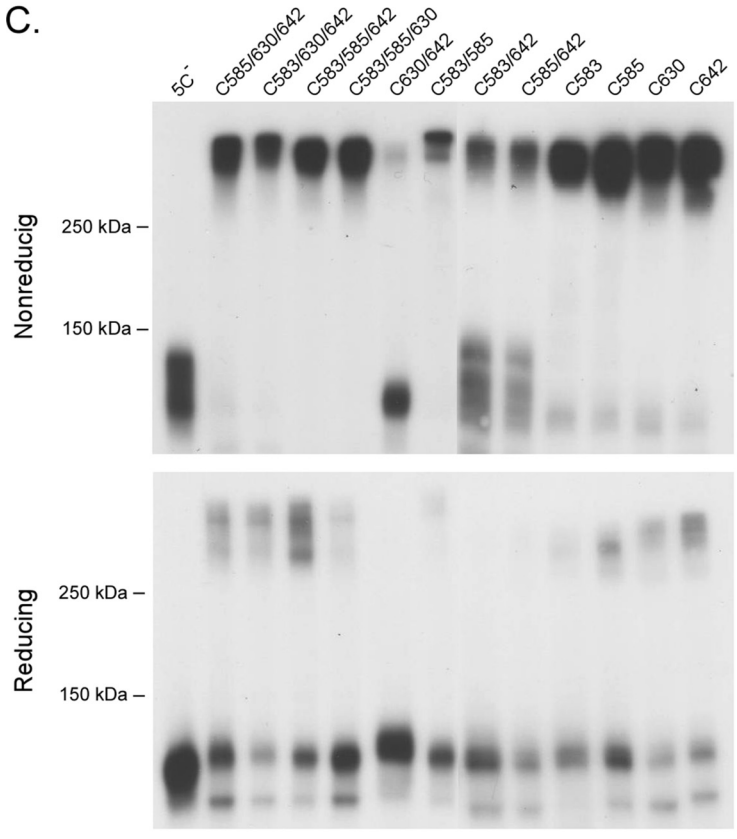

D.

Summary of BM labeling and dimerization of Cys combinations in EL-3

Cys combinations	BM (%)	BM (%) (+DTT)	Dimer
C1035	100	100	-
5C⁻	0	0	-
C585/630/642	0	100	+
C583/630/642	0	100	+
C583/585/642	0	100	+
C583/585/630	0	100	+
C630/642	0	100	-
C583/585	0	100	+
C583/642	20	100	+
C585/642	20	100	+
C583	0	100	+
C585	0	100	+
C630	0	100	+
C642	0	100	+

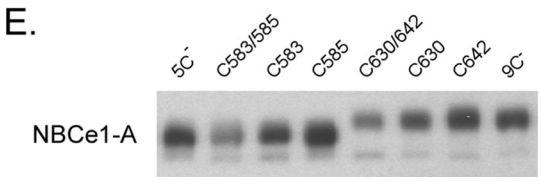

FIGURE 5. **BM labeling of cysteine combinations in NBCe1-A EL-3 and cross-linking analysis.** *A*, HEK 293 cells expressing various cysteine combinations were labeled with BM as described in Fig. 2. *Pro*, protein. *B*, HEK 293 cells expressing various cysteine combinations were washed twice with PBS and then incubated with 5 mM DTT at 37 °C for 30 min. Cells were then collected and washed three times with PBS prior to BM labeling. *C*, membranes isolated from HEK 293 cells expressing various cysteine combinations were resolved by 7.5% SDS-PAGE without (*upper panel*) and with β-ME treatment (*lower panel*). Protein bands above 250 kDa represent NBCe1-A dimers, and bands below 150 kDa represent NBCe1-A monomers. *D*, summary of BM labeling and cross-linking of the cysteine combinations in NBCe1-A EL-3. The level of biotin incorporation in each sample was quantified by densitometry, and the signal was normalized to the amount of NBCe1-A protein present in the sample. In each experiment, the level of biotinylation was compared with C1035, whose labeling was set to 100%. *E*, HEK 293 cells expressing various cysteine combinations were lysed, and NBCe1-A proteins were immunoprecipitated, resolved by 7.5% SDS-PAGE, transferred to a PVDF membrane, and probed with an anti-NBCe1-A antibody. Each experiment was performed at least three times.

functional effect (19). To determine the glycosylation status of NBCe1-A in mammalian cells, we individually substituted Asn^{592}, Asn^{597}, or Asn^{617} or simultaneously substituted $Asn^{597/617}$, $Asn^{592/617}$, $Asn^{592/597}$, or all three Asn sites with Gln in WT-NBCe1-A EL-3 and expressed these constructs in HEK 293 cells. Fig. 6*A* shows that NBCe1-A constructs with single glycosylation consensus site substitution all migrated at a similar molecular weight position as WT-NBCe1-A; with two consensus sites substitutions (except $Asn^{592/617}$), all migrated as a lower molecular weight band; and with three consensus sites substitutions, the proteins migrated as an even lower molecular weight band. Endo-F treatment completely elimi-

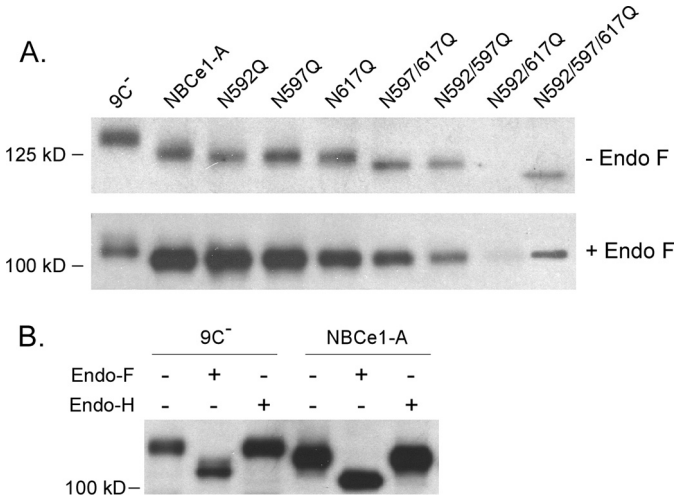

FIGURE 6. **Deglycosylation analysis of NBCe1-A with various Asn substitutions in EL-3.** *A*, plasma membranes of HEK 293 cells expressing various Asn substitutions in EL-3 were isolated, lysed in 2× SDS sample buffer with 2% β-ME, and resolved by 7.5% SDS-PAGE. A portion of the membrane pellet was lysed in Endo-F digestion buffer and incubated with Endo-F for 2 h at 37 °C following the manufacturer's protocol. Protein samples were then mixed with 2× SDS samples buffer with β-ME and processed as described above. *B*, membrane pellets containing either 9C⁻ or NBCe1-A were lysed in the Endo-F or Endo-H digestion buffer and digested with Endo-F or Endo-H following the manufacturer's protocol. Each experiment was performed at least three times.

nated the differences in protein migration of all the constructs except 9C⁻, indicating that the difference in protein migration is due to the presence of various numbers of complex glycans in NBCe1-A. This result also indicated that, in the absence of $Asn^{597/617}$, Asn^{592} became glycosylated. To test whether high mannose glycan is responsible for the slowed protein migration of Endo-F-treated 9C⁻, cell membranes containing 9C⁻ were isolated and treated with Endo-H at 37 °C for 2 h. Fig. 6*B* shows that Endo-F treatment significantly increased 9C⁻ migration on SDS-PAGE; however, Endo-H did not produce any effect. This result indicates that the difference in migration of Endo-F-treated 9C⁻ compared with the other constructs is likely due to an altered protein structure induced by high exposure of EL-3 on the NBCe1-A surface. Our data showed that when only Asn^{597} was present in EL-3, NBCe1-A protein was minimally expressed in the HEK 293 cells (Fig. 6*A*). We predict that this construct may have created a motif recognized by the endoplasmic reticulum-associated degradation pathway (28).

To determine whether *N*-glycosylation affects disulfide bond formation in EL-3, we compared the structural difference between 5C⁻ and the construct with N597Q/N617Q substitution (NBCe1-A-5C⁻-N597Q/N617Q (2N⁻-5C⁻)). Fig. 7*A* shows that in the absence of $Asn^{597/617}$ glycosylation none of the 4 cysteines in EL-3 were freely available for BM labeling. Moreover, NBCe1-A protein migrated as a monomer and was sensitive to β-ME reduction (Fig. 7*B*), suggesting that the formation of intramolecular disulfide bonds was not affected.

To examine whether *N*-glycosylation affects EL-3 folding, we tested the accessibility of the disulfide bonds in 2N⁻-5C⁻ to DTT reduction and chymotrypsin digestion as described above. Fig. 7, *C* and *D*, show that whole cell treatment with 5 mM DTT had minimal effect on 2N⁻-5C⁻ migration on SDS-PAGE; however, chymotrypsin (5-min) treatment released an N-terminal 75-kDa and a C-terminal 37-kDa protein band from 2N⁻-5C⁻, suggesting that EL-3 is less tightly folded when the two glycosylation sites are absent. The slow migration of the released N-terminal band in 2N⁻-5C⁻ (compared with that of 9C⁻) also suggested that Asn^{592} was glycosylated when the other two sites were absent.

We then tested whether *N*-glycosylation of EL-3 affects $Cys^{583/585}$ intermolecular cross-linking (in the absence of $Cys^{630/642}$). Fig. 7*E* shows that, when $Asn^{597/617}$ were substituted with Gln, $Cys^{583/585}$ migrated as a monomer, and surprisingly, when only the normally unglycosylated site Asn^{592} was substituted, $Cys^{583/585}$ migrated as a monomer. In contrast, substitution of $Asn^{597/617}$ or Asn^{592} with Gln had no detectable effect on Cys^{630}-Cys^{642} disulfide bonding (in the absence of $Cys^{583/585}$). Probing of these constructs with BM indicated that none of the cysteines were available for labeling (Fig. 7*F*), indicating that $Cys^{585/585}$ and $Cys^{630/642}$ form intramolecular disulfide bonds, respectively, under these conditions. Further analysis showed that all these constructs remained sensitive to Endo-F digestion (Fig. 7*G*), suggesting that $Asn^{597/617}$ were glycosylated in the absence of Asn^{592} and that Asn^{592} was glycosylated in the absence of $Asn^{597/617}$. Taken together, our findings suggest that a significant interplay between *N*-glycosylation and disulfide bonding of Cys^{583}-Cys^{585} exists that determines the conformation of this very large extracellular loop in NBCe1-A dimer.

EL-3 from Each NBCe1-A Monomer Is Closely Associated at the Dimeric Interface

EL-3 is predicted to be the largest extracellular loop on the surface of NBCe1-A. To clearly determine the size of EL-3, we individually substituted amino acids in the regions of Ala^{556}–Ser^{582} and Asn^{643}–Ser^{652} in 9C⁻ that cover the predicted linker regions between TM5 and EL-3 and between EL-3 and TM6. Whole cell labeling with BM was performed on all the constructs expressed in HEK 293 cells. Fig. 8, *A* and *B*, shows that the substituted cysteines D565C–S571C, N643C, and F644C but not P568C could be labeled only after the cells were treated with 5 mM DTT, suggesting they form intermolecular disulfide bonds precluding BM labeling. To verify this, we resolved NBCe1-A proteins under the nonreducing condition. Fig. 8*D* shows that the positive control C642 but not 5C⁻ was intermolecularly cross-linked to form an NBCe1-A dimer. Substituted cysteines in the regions of Y567C–N572C and N643C–D647C were cross-linked to form dimers, and cysteines in D565C–Y566C and I648C–L650C were not cross-linked. The slight difference in BM labeling and cross-linking is likely due to local structural constraints caused by protein folding. Based on the results of BM labeling (Fig. 8*C*) and protein cross-linking, we conclude that EL-3 contains 83 amino acids ranging from Asp^{565} to Asp^{647} (L562C was weakly labeled irrespective of reduction). The pattern of cross-linking also suggests that the extracellular ends of TM5 and TM6 from each of the respective monomers reside adjacently at the NBCe1-A dimeric interface.

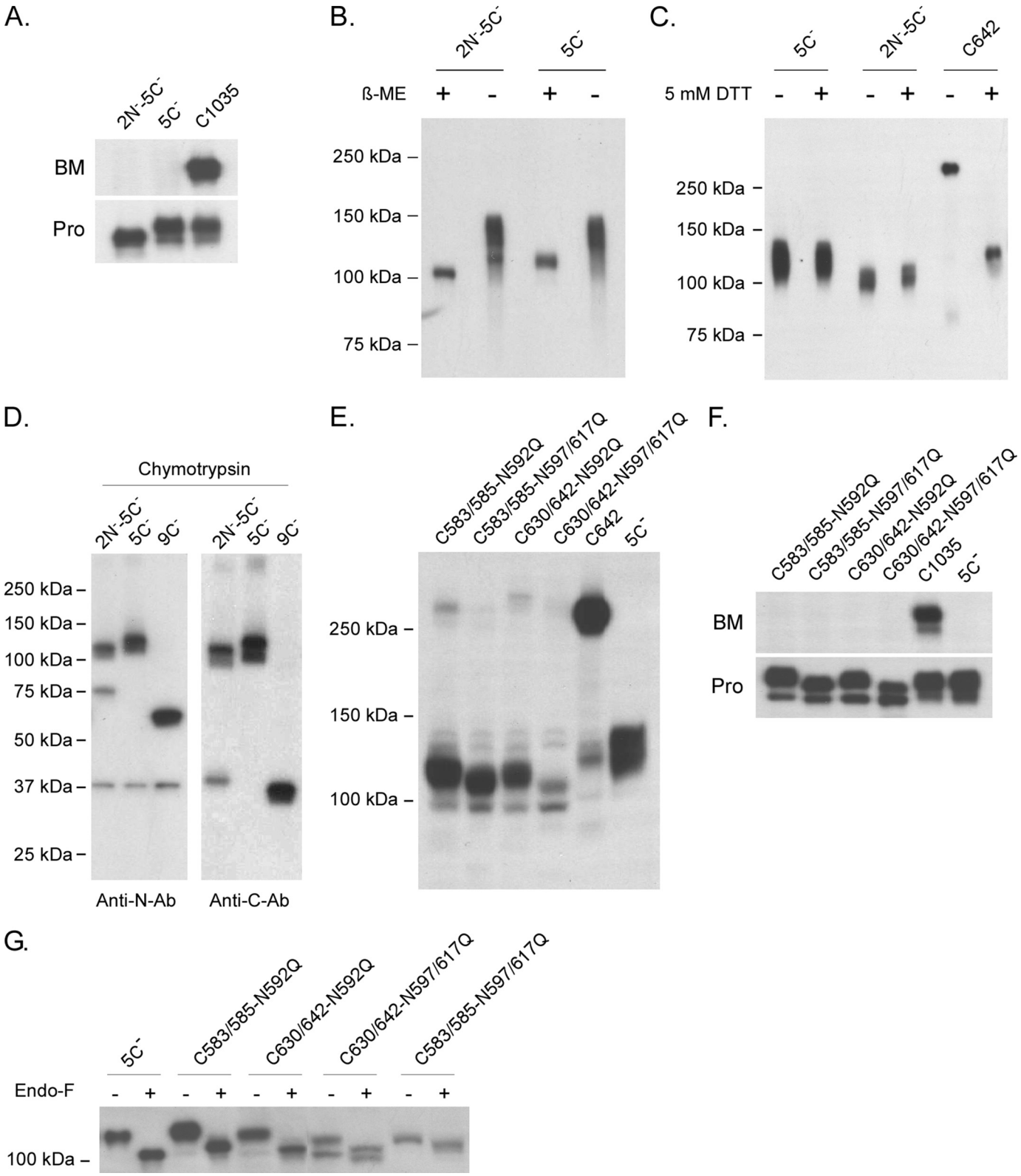

FIGURE 7. **Effect of *N*-glycosylation on disulfide bond formation in EL-3 and on topological folding of EL-3.** *A*, HEK 293 cells expressing $2N^{-}$-$5C^{-}$, $5C^{-}$, or C1035 were labeled with BM as described in Fig. 2. *Pro*, protein. *B*, the β-ME-treated and untreated $2N^{-}$-$5C^{-}$ and $5C^{-}$ protein samples were resolved by 7.5% SDS-PAGE, transferred to a PVDF membrane, and probed with an anti-NBCe1-A antibody. −, without β-ME; +, with β-ME. *C*, HEK cells expressing $5C^{-}$, $2N^{-}$-$5C^{-}$, or C642 were rinsed with PBS and incubated with 5 mM DTT at 37 °C for 30 min. Plasma membranes were then isolated, lysed in 2× SDS sample buffer without β-ME, and resolved by 7.5% SDS-PAGE. −, without DTT; +, with DTT. *D*, cell membranes from chymotrypsin-treated HEK 293 cells were isolated, resolved by 7.5% SDS-PAGE, and processed as described in Fig. 4 legend. *E*, cell membranes from HEK 293 cells expressing various cysteine combinations were isolated and resolved by 7.5% SDS-PAGE without β-ME treatment. *F*, representative data of BM labeling. The cysteine combinations were labeled with BM and processed as described in Fig. 2 legend. C1035 is the positive control; $5C^{-}$ is the negative control. *G*, representative data of Endo-F deglycosylation assay. Protein samples were processed as described in Fig. 6 legend. Each experiment was performed at least three times.

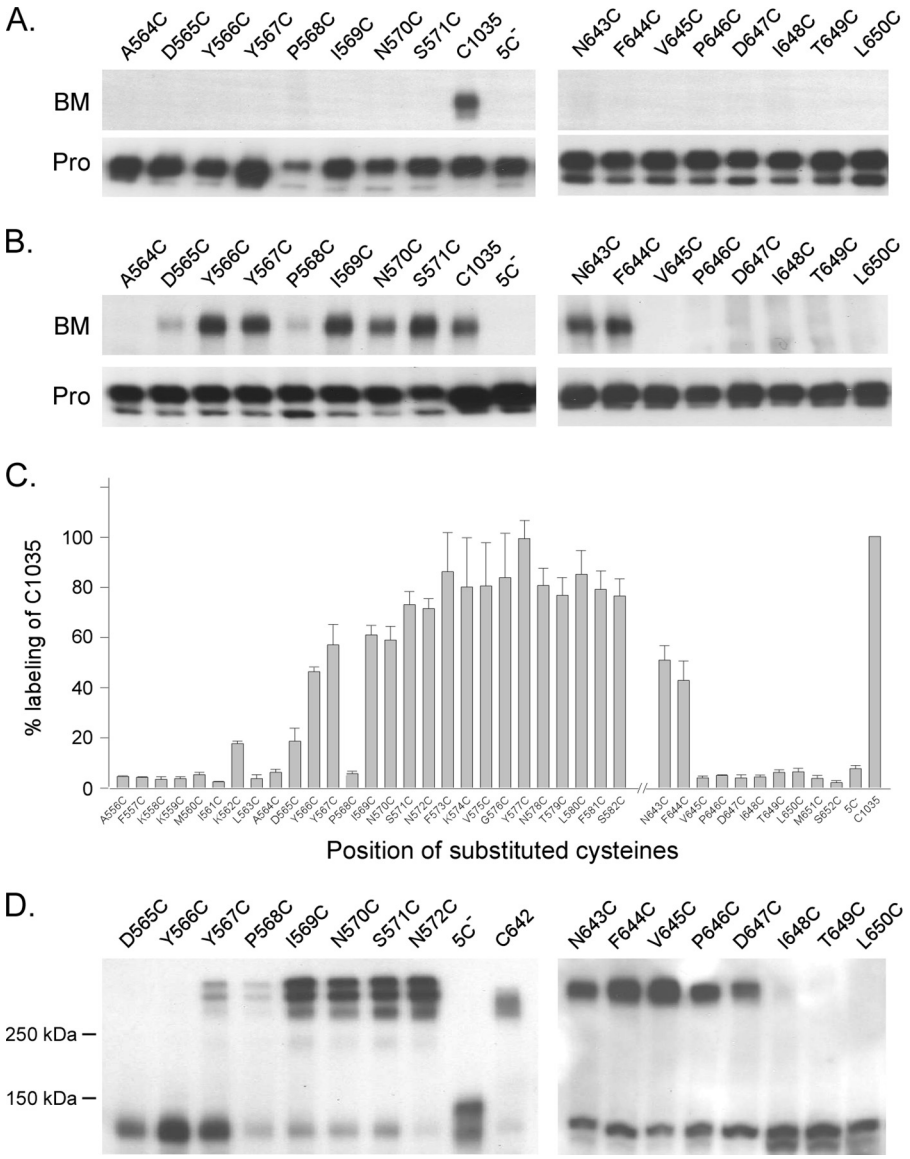

FIGURE 8. **BM labeling and spontaneous cross-linking of the cysteine substitutions in NBCe1-A EL-3.** *A*, representative BM labeling of substituted cysteines in EL-3. *B*, representative BM labeling of substituted cysteines in EL-3 after 5 mM DTT treatment. *Pro*, protein. *C*, summary of BM labeling after DTT treatment. The data were processed as described in Fig. 5 legend. The level of biotinylation was compared with C1035, whose labeling was set to 100%. *Error bars* represent mean ± S.E. (n = 5–7). *D*, representative cross-linking results of the substituted cysteines in EL-3. Protein bands above 250 kDa represent NBCe1-A dimer; bands below 150 kDa band represent NBCe1-A monomer.

Biological Importance of Disulfide Bonding in NBCe1-A EL-3

Lack of Disulfide Bonding in EL-3 Had No Effect on NBCe1-A Ion Transport—To assess whether the disulfide bonds in EL-3 are important for NBCe1-A ion transport, we removed the 4 cysteines in EL-3 (NBCe1-A-4C$^-$) and compared its base transport activity with WT-NBCe1-A. Transfected 293 cells were first equilibrated in a Na^+-free HEPES solution and then exposed to a Na^+-free HCO_3^--buffered CO_2-equilibrated solution. The rapid influx of CO_2 quickly lowered the intracellular pH (pH_i). Once pH_i had stabilized, the cells were bathed in Na^+-containing HCO_3^--buffered solution to drive NBCe1-A transport. Fig. 9, *A* and *B*, show that NBCe1-A-4C$^-$ transports base at a similar rate to that of WT-NBCe1-A, indicating that the disulfide bonding in EL-3 has no apparent effect on NBCe1-A total base transport in the HEK 293 cells.

We next tested whether the lack of disulfide bonds in EL-3 affects DIDS (the functional inhibitor of NBCe1-A) inhibition of the transporter. Fig. 9*B* shows that 1 mM DIDS treatment for 1 h inhibited both WT-NBCe1-A and NBCe1-A-4C$^-$ base transport to a similar level, suggesting that in the absence of disulfide bonds, the DIDS interaction site(s) has remained intact.

Effect of Abnormal Intermolecular Disulfide Bonding on NBCe1-A Ion Transport—To test whether proper disulfide bonding among the 4 cysteines in EL-3 is important for NBCe1-A ion transport, we analyzed the base transport of NBCe1-A constructs containing various cysteine combinations. Fig. 10*A* shows that substitution of any of the 4 cysteines or when only Cys^{583}, Cys^{585}, or both were present NBCe1-A transport function was dramatically impaired, but simultane-

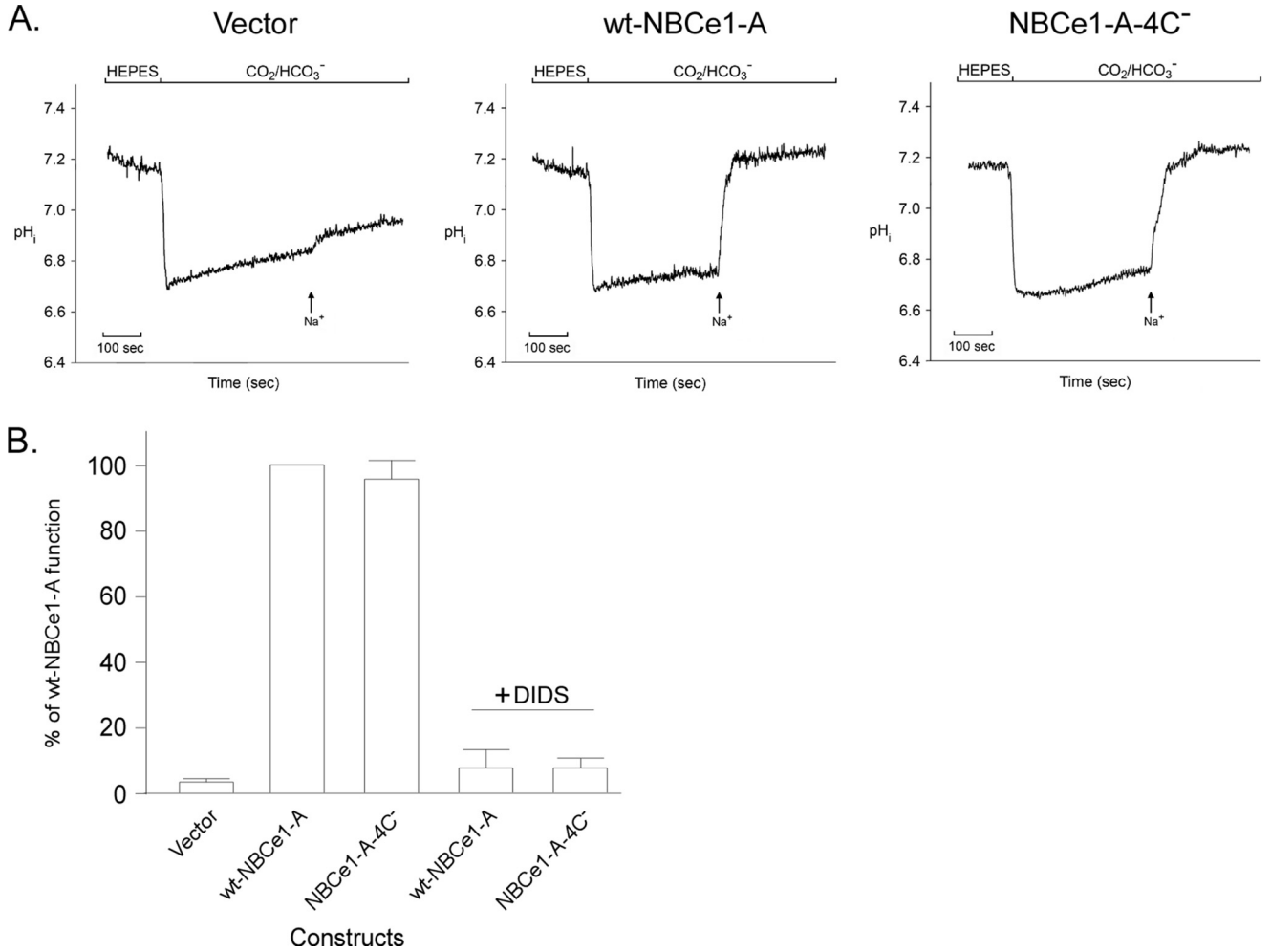

FIGURE 9. **Representative NBCe1-A transport assay.** *A*, HEK 293 cells grown on coverslips were transiently transfected with WT-NBCe1-A or NBCe1-A-4C^{-}, loaded with pH-sensitive probe BCECF-AM, and assayed with a microfluorometer. Cells were initially equilibrated in HEPES buffered-Na^+ free solution, and then intracellular pH was lowered by perfusing cells with a CO_2-HCO_3^- buffered-Na^+ free solution. Upon addition of a 140 mM Na^+-containing CO_2-HCO_3^--buffered solution, intracellular pH rapidly recovered in NBCe1-A-transfected cells but not in the mock-transfected cells. All solutions contained 30 μM 5′-(*N*-ethyl-*N*-isopropyl)amiloride to block endogenous Na^+/H^+ exchange. *B*, summary of the transport function of NBCe1-A and NBCe1-A-4C^{-} without and with DIDS treatment. For DIDS treatment, 1 mM DIDS was preincubated with cells expressing either WT-NBCe1-A or NBCe1-A-4C^{-} for 1 h at 37 °C in the 140 mM Na^+-containing CO_2-HCO_3^--buffered solution. Transport data are expressed as a percentage of WT-NBCe1-A function. *Error bars* represent mean ± S.E. (n = 5–7).

ous substitution of both Cys^{583} and Cys^{585} or when only Cys^{617}, Cys^{642}, or both were present, the transport function was significantly improved. These results indicate that intermolecular cross-linking between Cys^{583} and Cys^{585} on each monomer restricted the orientation or conformational changes of TM5 in NBCe1-A, which abrogated ion transport, suggesting that TM5 has an important role in NBCe1-A transport function.

Lack of Disulfide Bonding in EL-3 Had No Effect on NBCe1-A Membrane Stability—To determine whether the disulfide bonds in EL-3 affect NBCe1-A stability, a time course study of NBCe1-A-4C^{-} duration in the plasma membrane was performed. 24 h post-transfection, HEK 293 cells expressing either WT-NBCe1-A or NBCe1-A-4C^{-} were treated with cycloheximide to stop the protein production, and the level of both proteins in the plasma membrane was measured by protein surface labeling (25). Fig. 10, *B* and *C*, show that over a period of 96 h of monitoring, no difference could be detected in the surface protein level between these two constructs, suggesting that the stability of NBCe1-A protein in the plasma membrane is unaffected by the loss of EL-3 disulfide bonds.

DISCUSSION

In the present study, we scrutinized the structural importance of the 4 highly conserved cysteines to the topological folding of EL-3, the largest NBCe1-A extracellular loop. Our results demonstrated that the 4 cysteines form two intramolecular disulfide bonds constraining EL-3 in a uniquely folded conformation. This unique conformation is finely tuned by the presence of two *N*-glycosylations. Moreover, our findings demonstrate that the two EL-3 loops from each monomer reside closely at the NBCe1-A dimeric interface. This close association suggests that a unique domain-like structure is present on the NBCe1-A extracellular surface that potentially has an important physiological role related to NBCe1-A function.

Our results demonstrate clearly that interplay occurs between disulfide bonding and *N*-glycosylation in EL-3 that

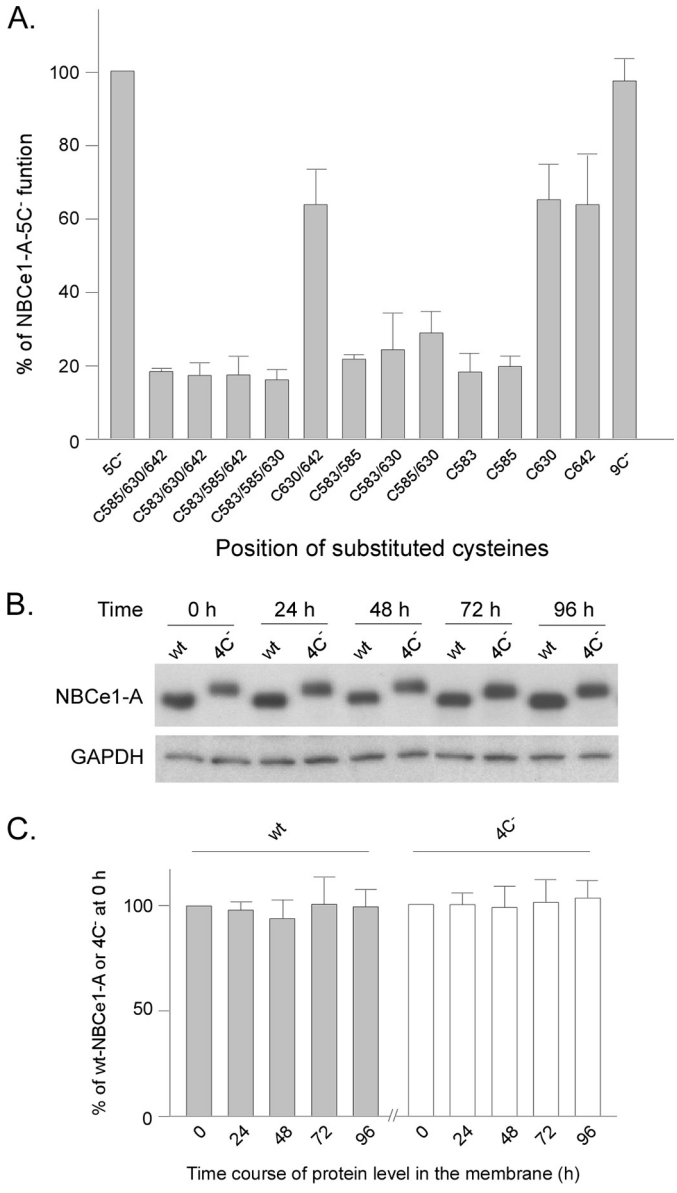

FIGURE 10. **Biological importance of disulfide bonding in NBCe1-A EL-3.** *A*, transport function of NBCe1-A with various cysteine combinations in NBCe1-A EL-3 was assayed as described in Fig. 9 legend. Transport data are expressed as a percentage of NBCe1-A-5C$^-$ function. *Error bars* represent mean ± S.E. (n = 6–7). *B*, representative data of NBCe1-A protein surface labeling after cycloheximide treatment. 24 h post-transfection, cells expressing WT-NBCe1-A or NBCe1-A-4C$^-$ were incubated with cycloheximide (10 μM) in fresh cell culture medium. At 0, 24, 48, 72, and 96 h post-cycloheximide treatment, the cells were rinsed with PBS and incubated with sulfo-NHS-SS-biotin for 30 min at 4 °C following the manufacturer's protocol. GAPDH was used as an internal standard. *C*, summary of sulfo-NHS-SS-biotin surface labeling assay. The level of NBCe1-A protein in each sample was quantified by densitometry and compared with the protein level at 0 h post-cycloheximide treatment. *Error bars* represent mean ± S.E. (n = 3).

determines the topological folding of this large extracellular loop. This conclusion is supported by the following findings. 1) The 4 cysteines in EL-3 form two intramolecular disulfide bonds, Cys^{583}-Cys^{585} and Cys^{630}-Cys^{642}, respectively, restraining EL-3 in a folded conformation. 2) When one or both of the two disulfide bonds are absent, EL-3 adopts an extended conformation highly accessible to DTT reduction or chymotrypsin digestion. 3) The two disulfide bonds are folded in the NBCe1-A protein, unexposed to the extracellular medium, even after 1 M Na_2CO_3 and 50 mM DTT treatment. 4) The correct formation of the first disulfide bond is dependent on the presence of the second disulfide bond. 5) When the second disulfide bond is absent, the correct formation of the first disulfide bond is suppressed by the presence of *N*-glycosylation at Asn^{592}, Asn^{597}, and Asn^{617}. 6) When the two *N*-glycosylation sites Asn^{597} and Asn^{617} were absent, EL-3 became less tightly folded and was accessible to chymotrypsin digestion. These findings indicate that a complex enzymatic orchestration must exist between *N*-glycosylation and disulfide bond-forming enzymes in the endoplasmic reticulum that determines the final folding of EL-3 during NBCe1-A protein maturation.

Our data have also shown that EL-3 contains 83 amino acids ranging from Asp^{565} to Asp^{647}. This large extracellular loop is in a folded conformation restrained by the two native disulfide bonds. The formation of the second disulfide bond (Cys^{630}-Cys^{642}) is spontaneous and unaffected by the *N*-glycosylation state of EL-3 or the first disulfide bond, whereas formation of the first disulfide bond (Cys^{583}-Cys^{585}) is dependent on the presence of the second disulfide bond. When Cys^{630} and Cys^{642} were absent, Cys^{583} and Cys^{585} became intermolecularly cross-linked, forming a reduction-sensitive NBCe1-A dimer. Interestingly, when only 1 of the 4 cysteines was present in EL-3, it also cross-linked to itself on the opposite monomer to form a reduction-sensitive NBCe1-A dimer. These results demonstrate that the two disulfide bonds work synergistically to control EL-3 in a folded conformation, thereby structuring the topological surface of NBCe1-A dimer.

EL-3 contains three *N*-glycosylation consensus sites, but only two are glycosylated in the plasma membrane processed NBCe1-A (19). Our data determined that Asn^{592} became glycosylated when either Asn^{597}, Asn^{617}, or both were absent or when both of the cysteines at 583 and 585 were absent. The simplest explanation is that Asn^{592} is initially glycosylated in the endoplasmic reticulum catalyzed by the oligosaccharyltransferase, and during protein maturation, the glycan is enzymatically removed. Indeed, the oligosaccharyltransferase subunits Ost3p and Ost6p were shown to have oxidoreductase activity (29), which would prevent the disulfide bond formation between Cys^{583} and Cys^{585} during protein synthesis that allows efficient glycosylation at Asn^{592}. Our data are compatible with the hypothesis that the first disulfide bond and glycans at Asn^{597} and Asn^{617} form a three-dimensional motif that is required for an endoglycosidase to recognize and remove the complex glycan at Asn^{592}. When any of these three requirements is missing, the glycosidase is unable to recognize this site and subsequently unable to remove the glycan at Asn^{592}. We predict that this process must have occurred in the second stage of membrane protein folding during NBCe1-A dimerization. The detailed enzymatic mechanisms behind this phenomenon require further investigation but clearly have potential general relevance to the biosynthesis of membrane proteins that have a structural and/or functional requirement of *N*-glycosylation and disulfide bond formation.

One of the major findings in the present study is that each of the substituted cysteines was cross-linked to the corresponding residue on the opposite monomer. The spontaneous intermo-

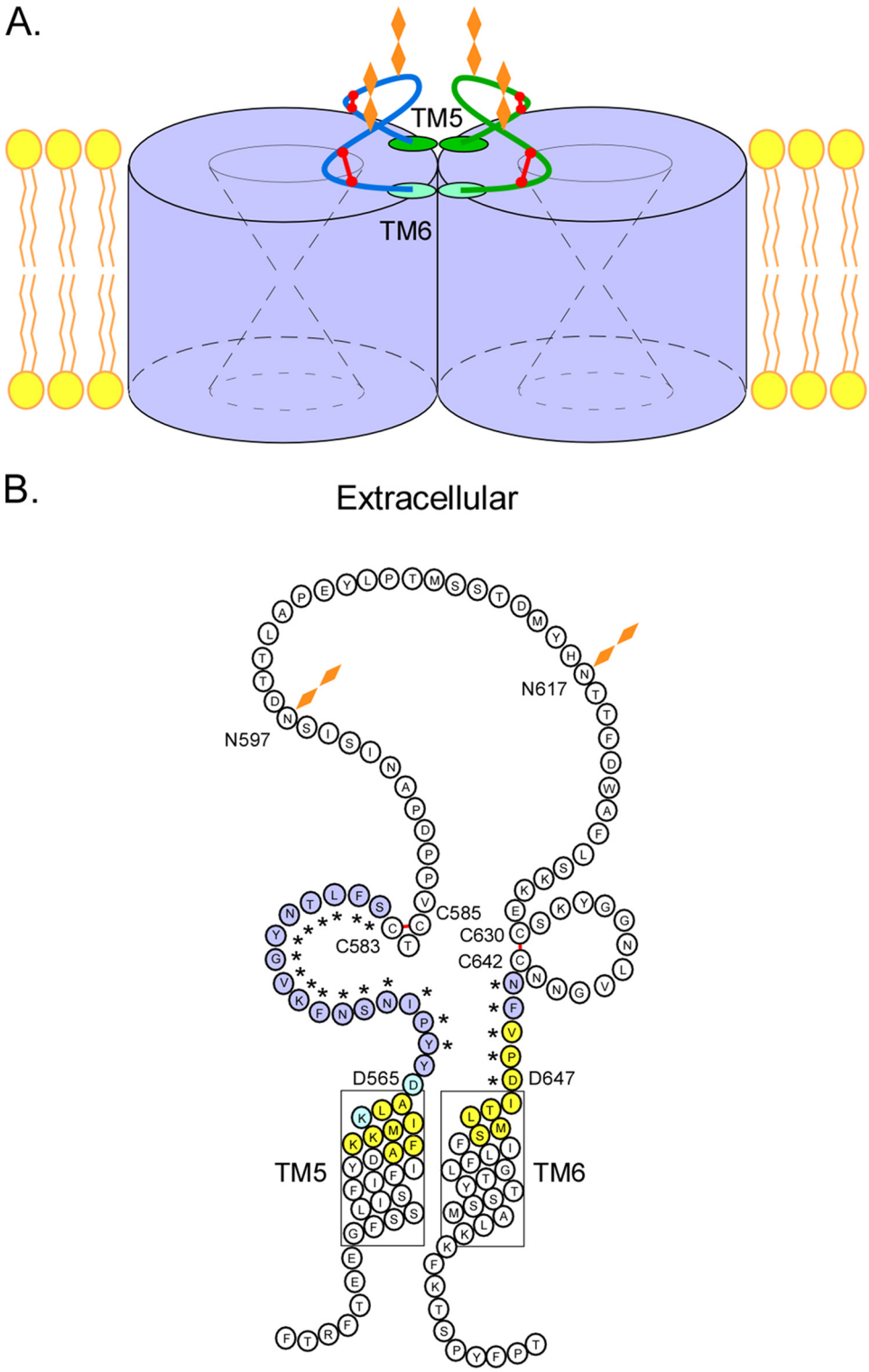

FIGURE 11. **Proposed topological folding of NBCe1-A EL-3.** *A*, EL-3 from each NBCe1-A monomer resides closely at the dimeric interface with the extracellular ends of TM5 and TM6 located adjacently. Each EL-3 is folded in a unique conformation restricted by the two disulfide bonds (*red line*). The two *N*-glycosylation sites are indicated as *brown diamonds*. *B*, detailed topological folding of EL-3. The two *N*-glycosylation sites are shown as *brown diamonds*; two disulfide bonds are shown as *red lines*; strongly BM-labeled substituted cysteine residues (after DTT treatment) are shown in *blue* , weakly labeled residues are shown in *light blue* (K562C was also weakly labeled without DTT treatment), and unlabeled residues are shown in *yellow*; and substituted cysteines forming cross-linked NBCe1-A dimers are indicated by *asterisks*.

lecular cross-linking requires the 2 cysteines to be in close proximity, indicating that EL-3 from each of the monomers resides closely at the dimeric interface and that the extracellular ends of TM5 or -6 from each monomer are adjacently located. Upon closer examination, we observed an almost evenly distributed number of amino acids (~12) between TM5 and the first disulfide bond, the first disulfide bond and Asn^{597}, Asn^{617} and the second disulfide bond, and Cys^{630} and Cys^{642}. This unique pat-

tern of amino acid distribution indicates that EL-3 folds like a "clover" on the surface of NBCe1-A at the dimeric interface (Fig. 11, *A* and *B*). The adjacent parallel location of two symmetrically folded EL-3s from each monomer resembles a domain-like structure on the NBCe1-A extracellular surface.

Disulfide bonds in a transmembrane protein are known to be important for protein structural stabilization and thermodynamics (30). However, our data indicated that NBCe1-A lacking the disulfide bonds in EL-3 had a similar membrane stability compared with WT-NBCe1-A, suggesting that the disulfide bonds in EL-3 do not contribute to the core structural folding of the transporter but rather define the extracellular surface topography.

Disulfide bonding on the surface of the human organic cation transporter 2 and the Cys-loop ligand-gated ion channel receptors was shown to have critical functional roles (20, 21). Our functional assay showed that presence or absence of the two disulfide bonds in EL-3 had no demonstrable effect on NBCe1-A base transport, indicating that in the heterologous expression system the two disulfide bonds in EL-3 do not affect the baseline NBCe1-A base transport activity. Interestingly, our functional assay also showed that intermolecular cross-linking between the mispaired cysteines at 583 or 585 but not at 630 or 642 dramatically impaired the base transport function, suggesting that restriction of the normal orientation or conformational changes of TM5 abrogates NBCe1-A ion transport. It is known that DIDS interacts with the peptide motif ^{558}KKMIK^{562} in TM5 close to the beginning of EL-3 (22) and that D555E substitution in TM5 converts NBCe1-A from a transporter to an anion channel (23). Our findings provide further support that TM5 has a critical role in NBCe1-A base transport.

REFERENCES

1. Kurtz, I., and Zhu, Q. (2013) Proximal renal tubular acidosis mediated by mutations in NBCe1-A: unraveling the transporter's structure-functional properties. *Front. Physiol.* **4,** 350
2. Kurtz, I. (2013) in *Seldin and Giebisch's The Kidney: Physiology and Pathophysiology* (Alperin, R. J., Caplan, M., and Moe, O.W., eds) 5th Ed., pp. 1837–1860, Elsevier/Academic Press, Amsterdam
3. Parker, M. D., and Boron, W. F. (2013) The divergence, actions, roles, and relatives of sodium-coupled bicarbonate transporters. *Physiol. Rev.* **93,** 803–959
4. Seki, G., Horita, S., Suzuki, M., Yamazaki, O., Usui, T., Nakamura, M., and Yamada, H. (2013) Molecular mechanisms of renal and extrarenal manifestations caused by inactivation of the electrogenic Na^+-HCO_3^- cotransporter NBCe1. *Front. Physiol.* **4,** 270
5. Zhu, Q., Kao, L., Azimov, R., Newman, D., Liu, W., Pushkin, A., Abuladze, N., and Kurtz, I. (2010) Topological location and structural importance of the NBCe1-A residues mutated in proximal renal tubular acidosis. *J. Biol. Chem.* **285,** 13416–13426
6. Zhu, Q., Shao, X. M., Kao, L., Azimov, R., Weinstein, A. M., Newman, D., Liu, W., and Kurtz, I. (2013) Missense mutation T485S alters NBCe1-A electrogenicity causing proximal renal tubular acidosis. *Am. J. Physiol. Cell Physiol.* **305,** C392–C405
7. Abuladze, N., Song, M., Pushkin, A., Newman, D., Lee, I., Nicholas, S., and Kurtz, I. (2000) Structural organization of the human NBC1 gene: kNBC1 is transcribed from an alternative promoter in intron 3. *Gene* **251,** 109–122
8. McAlear, S. D., Liu, X., Williams, J. B., McNicholas-Bevensee, C. M., and Bevensee, M. O. (2006) Electrogenic Na/HCO_3 cotransporter (NBCe1) variants expressed in *Xenopus* oocytes: functional comparison and roles of the amino and carboxy termini. *J. Gen. Physiol.* **127,** 639–658
9. Liu, Y., Xu, J. Y., Wang, D. K., Wang, L., and Chen, L. M. (2011) Cloning and identification of two novel NBCe1 splice variants from mouse reproductive tract tissues: a comparative study of NCBT genes. *Genomics* **98,** 112–119
10. Kao, L., Sassani, P., Azimov, R., Pushkin, A., Abuladze, N., Peti-Peterdi, J., Liu, W., Newman, D., and Kurtz, I. (2008) Oligomeric structure and minimal functional unit of the electrogenic sodium bicarbonate cotransporter NBCe1-A. *J. Biol. Chem.* **283,** 26782–26794
11. Zhu, Q., Liu, W., Kao, L., Azimov, R., Newman, D., Abuladze, N., and Kurtz, I. (2013) Topology of NBCe1 protein transmembrane segment 1 and structural effect of proximal renal tubular acidosis (pRTA) S427L mutation. *J. Biol. Chem.* **288,** 7894–7906
12. Zhu, Q., Kao, L., Azimov, R., Abuladze, N., Newman, D., Pushkin, A., Liu, W., Chang, C., and Kurtz, I. (2010) Structural and functional characterization of the C-terminal transmembrane region of NBCe1-A. *J. Biol. Chem.* **285,** 37178–37187
13. Li, H. C., Worrell, R. T., Matthews, J. B., Husseinzadeh, H., Neumeier, L., Petrovic, S., Conforti, L., and Soleimani, M. (2004) Identification of a carboxyl-terminal motif essential for the targeting of Na^+-HCO_3^- cotransporter NBC1 to the basolateral membrane. *J. Biol. Chem.* **279,** 43190–43197
14. Li, H. C., Li, E. Y., Neumeier, L., Conforti, L., and Soleimani, M. (2007) Identification of a novel signal in the cytoplasmic tail of the Na^+:HCO_3^- cotransporter NBC1 that mediates basolateral targeting. *Am. J. Physiol. Renal Physiol.* **292,** F1245–F1255
15. Suzuki, M., Van Paesschen, W., Stalmans, I., Horita, S., Yamada, H., Bergmans, B. A., Legius, E., Riant, F., De Jonghe, P., Li, Y., Sekine, T., Igarashi, T., Fujimoto, I., Mikoshiba, K., Shimadzu, M., Shiohara, M., Braverman, N., Al-Gazali, L., Fujita, T., and Seki, G. (2010) Defective membrane expression of the Na^+-HCO_3^- cotransporter NBCe1 is associated with familial migraine. *Proc. Natl. Acad. Sci. U.S.A.* **107,** 15963–15968
16. Zhu, Q., Kao, L., Newman, D., and Kurtz, I. (2010) The C-terminal tail of the NBCe1-A dimer is structured: relevance to CAII binding. *J. Am. Soc. Nephrol.* **21,** 251A
17. Zhu, Q., Azimov, R., Kao, L., Newman, D., Liu, W., Abuladze, N., Pushkin, A., and Kurtz, I. (2009) NBCe1-A transmembrane segment 1 lines the ion translocation pathway. *J. Biol. Chem.* **284,** 8918–8929
18. McAlear, S. D., and Bevensee, M. O. (2006) A cysteine-scanning mutagenesis study of transmembrane domain 8 of the electrogenic sodium/bicarbonate cotransporter NBCe1. *J. Biol. Chem.* **281,** 32417–32427
19. Choi, I., Hu, L., Rojas, J. D., Schmitt, B. M., and Boron, W. F. (2003) Role of glycosylation in the renal electrogenic Na^+-HCO_3^- cotransporter (NBCe1). *Am. J. Physiol. Renal Physiol.* **284,** F1199–F1206
20. Brast, S., Grabner, A., Sucic, S., Sitte, H. H., Hermann, E., Pavenstädt, H., Schlatter, E., and Ciarimboli, G. (2012) The cysteines of the extracellular loop are crucial for trafficking of human organic cation transporter 2 to the plasma membrane and are involved in oligomerization. *FASEB J.* **26,** 976–986
21. Blum, A. P., Gleitsman, K. R., Lester, H. A., and Dougherty, D. A. (2011) Evidence for an extended hydrogen bond network in the binding site of the nicotinic receptor: role of the vicinal disulfide of the α1 subunit. *J. Biol. Chem.* **286,** 32251–32258
22. Lu, J., and Boron, W. F. (2007) Reversible and irreversible interactions of DIDS with the human electrogenic Na/HCO_3 cotransporter NBCe1-A: role of lysines in the KKMIK motif of TM5. *Am. J. Physiol. Cell Physiol.* **292,** C1787–C1798
23. Yang, H. S., Kim, E., Lee, S., Park, H. J., Cooper, D. S., Rajbhandari, I., and Choi, I. (2009) Mutation of aspartate 555 of the sodium/bicarbonate transporter SLC4A4/NBCe1 induces chloride transport. *J. Biol. Chem.* **284,** 15970–15979
24. Bok, D., Schibler, M. J., Pushkin, A., Sassani, P., Abuladze, N., Naser, Z., and Kurtz, I. (2001) Immunolocalization of electrogenic sodium-bicarbonate cotransporters pNBC1 and kNBC1 in the rat eye. *Am. J. Physiol. Renal Physiol.* **281,** F920–F935
25. Patterson, S. T., and Reithmeier, R. A. (2010) Cell surface rescue of kidney anion exchanger 1 mutants by disruption of chaperone interactions. *J. Biol. Chem.* **285,** 33423–33434
26. Zhu, Q., Lee, D. W., and Casey, J. R. (2003) Novel topology in C-terminal

region of the human plasma membrane anion exchanger, AE1. *J. Biol. Chem.* **278,** 3112–3120
27. Zhu, Q., and Casey, J. R. (2007) Topology of transmembrane proteins by scanning cysteine accessibility mutagenesis methodology. *Methods* **41,** 439–450
28. Vembar, S. S., and Brodsky, J. L. (2008) One step at a time: endoplasmic reticulum-associated degradation. *Nat. Rev. Mol. Cell Biol.* **9,** 944–957
29. Schulz, B. L., Stirnimann, C. U., Grimshaw, J. P., Brozzo, M. S., Fritsch, F., Mohorko, E., Capitani, G., Glockshuber, R., Grütter, M. G., and Aebi, M. (2009) Oxidoreductase activity of oligosaccharyltransferase subunits Ost3p and Ost6p defines site-specific glycosylation efficiency. *Proc. Natl. Acad. Sci. U.S.A.* **106,** 11061–11066
30. Fass, D. (2012) Disulfide bonding in protein biophysics. *Annu. Rev. Biophys.* **41,** 63–79